The Multiport Communication Theory

Michel T. Ivrlač and Josef A. Nossek

Abstract

Information theory serves well as the *mathematical* theory of communication. However, it contains no provision that makes sure its theorems are consistent with the physical laws that govern any existing realization of a communication system. Therefore, it may not be surprising that applications of information theory or signal processing, as currently practiced, easily turn out to be *inconsistent* with fundamental principles of physics, such as the law of conservation of energy. It is the purpose of *multiport communication* theory to provide the necessary framework ensuring that applications of signal processing and information theory actually do comply with physical law. This framework involves a circuit theoretic approach where the inputs and outputs of the communication system are associated with ports of a multiport black-box. Thanks to each port being described by a *pair* of two instead of just one variable, consistency with physics can be maintained. The connection to information theory and signal processing is then obtained by means of isomorphisms between mathematical (formal) symbols of the latter and the physical quantities of the multiport model. In this article, the principles of the multiport communication theory are presented and accompanied by a discussion of a number of interesting results of its application to single and multi-antenna radio communications in single- and multi-user contexts.

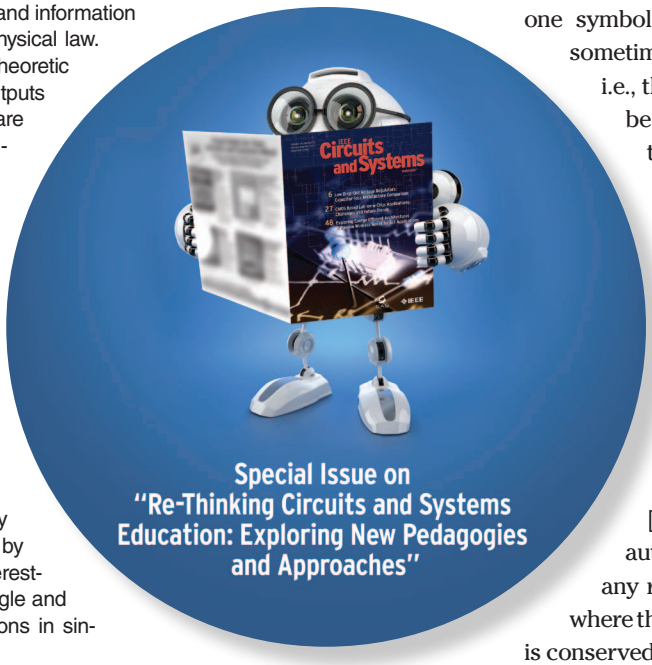

IMAGE LICENSED BY INGRAM PUBLISHING

I. Introduction

There exist a number of fundamental principles in physics which can be stated as conservation laws, meaning that there are quantities which can be calculated for a physical system at one time, and when recalculated at a later time come out the same [1]. An example is the law of conservation of energy. Frequently, application of these laws help in arriving at elegant solutions of complicated problems. For instance, the motion of planets around the sun can be obtained solely by following the implications of the laws of conservation of energy and angular momentum [2]. Moreover, the conservation laws are also deep principles for they relate to symmetry in physics [3]. For instance, conservation of energy implies that the laws of Nature are time-invariant, and vice versa.

Also in signal processing and information theory, the concept of energy is a prominent one. It appears as the energy required to transfer one bit of information, or one symbol of the signal alphabet, or sometimes in form of transmit power, i.e., the rate at which energy must be supplied per unit of time to keep the communication going. Yet, it is interesting that the fact that energy is conserved, this very fact that is of such fundamental importance in physics, apparently plays *no* role in standard textbooks on information theory [4], signal processing [5], communication theory [6] or signal theory [7]. The authors are also not aware of any research work in these areas where the remarkable fact that energy is conserved is explored or discussed.

The reason for this strange absence of conservation laws in signal processing, information theory and related disciplines seems to be the fact that inputs and outputs are described by single variables each, instead of by a pair of conjugated variables, like position and momentum in Hamiltonian mechanics [3], or voltage and current in circuit theory [8]. Such conjugated pairs are, however, necessary to capture the notion of energy or power and, by virtue of the fluctuation-dissipation theorem [9], the notion of thermal equilibrium noise.

The absence of conjugated pairs in information theory and signal processing shows that they are ill equipped to handle fundamental concepts such as energy, power

Digital Object Identifier 10.1109/MCAS.2014.2333618
Date of publication: 20 August 2014

In signal processing and information theory, the concept of energy is a prominent one. It appears as the energy required to transfer one bit of information, or one symbol of the signal alphabet, or sometimes in form of transmit power.

and noise in any way consistent with physics. This is the point where the *multiport communication theory* comes into the play. It establishes an interface between the physical world which uses conjugated pairs, and the information world, which uses only half the number of variables. Thereby it restores physical consistency and, thus, ensures the applicability of those mathematical theories of communication to the physical world.

After elaborating a little bit on making mathematical models consistent with physics, we describe the principles of multiport communications and finally present results of its application to multi-antenna radio communication systems. In particular, the results on *array gain*, *diversity*, *spatial multiplexing* and *space division multiple access* are presented, and may turn out to be rather surprising.

II. Physical Meaning and Consistency

A. Scalar Signals and One-Ports

Scalar signals occurring in information processing and communication systems are usually either complex valued continuous functions of time, $x(t) \in \mathbb{C}$, or sequences $x[k] \in \mathbb{C}$ of complex numbers. The instantaneous power is in most textbooks (e.g., [6], [10], [11]) defined as:

$$P(t) = |x(t)|^2, \quad P[k] = |x[k]|^2. \tag{1}$$

In the case that x is a random variable, it is conventional to apply the expectation operation to arrive at the average power $P_{\text{av}} = \mathrm{E}[P[k]]$. The physical power flowing into a one-port is given by:

$$P_{\text{phy}}(t) = u(t) \cdot i(t) = u^2(t)/R = i^2(t) \cdot R, \tag{2}$$

where we have assumed that the port is terminated by a passive linear resistor $R > 0$. In this specific case, the signal power (1) is *strictly proportional* to the physical power (2) provided that an *isomorphism* between signals and physical quantities is made in one of the following ways:

$$\left.\begin{array}{ll} & x(t) \sim u(t) \\ \text{or} & x(t) \sim i(t) \\ \text{or} & x(t) \sim (\alpha u(t) + \beta i(t)) \end{array}\right\} \Rightarrow P(t) \sim P_{\text{phy}}(t).$$

Therefore, the question »what does the signal $x(t)$ mean physically?« is of secondary interest in this case. The standard textbook definition of signal power and signal energy can be applied and there is no conflict.

B. Vector Signals and Multi-Ports

Let us now consider a vector signal $\boldsymbol{x}(t) \in \mathbb{C}^n$, or $\boldsymbol{x}[k] \in \mathbb{C}^n$, the instantaneous power of which is usually defined as:

$$P(t) = \|\boldsymbol{x}(t)\|_2^2, \quad P[k] = \|\boldsymbol{x}[k]\|_2^2. \tag{3}$$

The physical power which flows into a multi-port is equal to the sum of the powers flowing through the ports. Let us show with a simple example with only two ports, that it is not possible to have a simple assignment of signals to physical quantities, as was possible in the scalar case. The physical power which flows into the two-port in Figure 1 turns out to be

$$P_{\text{phy}}(t) = 2R(i_1^2 + i_2^2 + i_1 i_2) = \frac{2}{3}(u_1^2 + u_2^2 - u_1 u_2)/R. \tag{4}$$

Even in this simple case, signal power (3) is *not* proportional to physical power (4), no matter which of the following isomorphisms between the vector signal $\boldsymbol{x}(t)$ and the physical quantities $\boldsymbol{u}(t) = [u_1(t)\, u_2(t)]^{\mathrm{T}}$ or $\boldsymbol{i}(t) = [i_1(t)\ i_2(t)]^{\mathrm{T}}$ we may choose:

$$\left.\begin{array}{ll} & \boldsymbol{x}(t) \sim \boldsymbol{u}(t) \\ \text{or} & \boldsymbol{x}(t) \sim \boldsymbol{i}(t) \\ \text{or} & \boldsymbol{x}(t) \sim (\alpha \boldsymbol{u}(t) + \beta \boldsymbol{i}(t)) \end{array}\right\} \Rightarrow P(t) \nsim P_{\text{phy}}(t).$$

Nevertheless, it is possible to save the conventional way (3) of computing power using the isomorphism

$$\boldsymbol{x}(t) \sim \begin{bmatrix} u_1(t) + \alpha u_2(t) \\ \alpha u_1(t) + u_2(t) \end{bmatrix}, \quad \text{with } \alpha \in \{-2 \pm \sqrt{3}\}.$$

This does make the signal power strictly proportional to physical power. But obviously this isomorphism was exactly tailored to the two-port in question. For other two-ports it usually would have to be different. Therefore, and in contrast to the case of scalar signals, the isomorphism is important. Let us, therefore, have a closer look into the isomorphisms and their implications.

Michel T. Ivrlač and Josef A. Nossek are with the Institute for Circuit Theory and Signal Processing, Technische Universität München, e-mails: {nossek,ivrlac}@ tum.de.

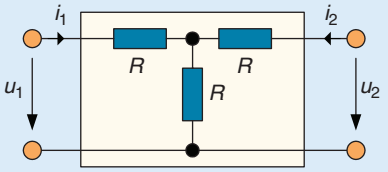

Figure 1. Resistive, passive ($R > 0$) two-port.

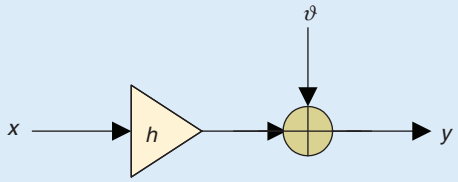

Figure 3. A simple mathematical system model.

C. Implications of Isomorphisms

Any mathematical system model can be made consistent with the governing physics by following a two step procedure. At first, meaning is assigned to the formal symbols of the mathematical model by creating an *isomorphism* with physical quantities. Once this identification of formal symbols with physical quantities is made, all applicable physical laws and technical constraints that govern the relationship between those physical quantities are going to imply certain relationships between the formal symbols of the mathematical model. Thus, the second task is to find out all the relevant *implications* of the chosen isomorphism. The whole process is shown in Figure 2. To illustrate this rather abstract points let us have a look at a simple but illuminating example.

Figure 3 shows an additive white Gaußian noise channel with input signal x, output signal y, channel coefficient h, and additive, zero-mean, white Gaußian noise ϑ with variance σ_ϑ^2. It can serve as a simple incarnation of a mathematical model of a communication system. A key parameter that can be extracted from this model is the signal to noise ratio

$$\mathrm{SNR} = \frac{\mathrm{E}\left[|y|^2 \mid \vartheta = 0\right]}{\mathrm{E}\left[|y|^2 \mid x = 0\right]} = \mathrm{E}\left[|x|^2\right] \cdot \frac{|h|^2}{\sigma_\vartheta^2}. \tag{5}$$

If the magnitude of the channel coefficient h is reduced by a factor of 2 we would expect a reduction of SNR by a factor of 4 as predicted by (5). But that would only be true if σ_ϑ^2 is independent of h. However, as soon as we assign physical meaning to this model there arises a certain relationship between σ_ϑ^2 and h. It is actually this relationship that constitutes the essence of the model. To illustrate this point, let us assume that Figure 3 shall be used to model an idealized physical communication system whose circuit model is shown in Figure 4. It consists of an ideal transformer that is driven by a voltage source with voltage u_G and source resistance R, and terminated with a load resistance R, both resistances subject to thermal equilibrium noise represented by the two current sources with zero mean and variance of σ_0^2. The noise sources are uncorrelated with each other. The voltage transformation ratio, $\ddot{u}$, shall be variable between 0 and 1. Let the simple isomorphism:

$$x = u_\mathrm{G}, \quad y = u_\mathrm{L}, \tag{6}$$

establish the correspondence between the mathematical model from Figure 3, and the circuit from Figure 4. Circuit analysis then reveals with

$$\sigma_\vartheta^2 = \left(1 - \sqrt{1 - 4h^2}\right)\sigma_0^2/2, \tag{7}$$

a peculiar relationship between the channel coefficient h and the variance σ_ϑ^2 of the additive noise. Therefore, (7) is an implication of the isomorphism (6). Another implication is that $|h| \le 1/2$ must hold true, because σ_ϑ^2 must be real-valued. Finally, using (7) in (5), we obtain the most intriguing implication. As shown in Figure 5, the SNR keeps increasing with decreasing magnitude of the channel coefficient! How absurd it gets! Yet, this

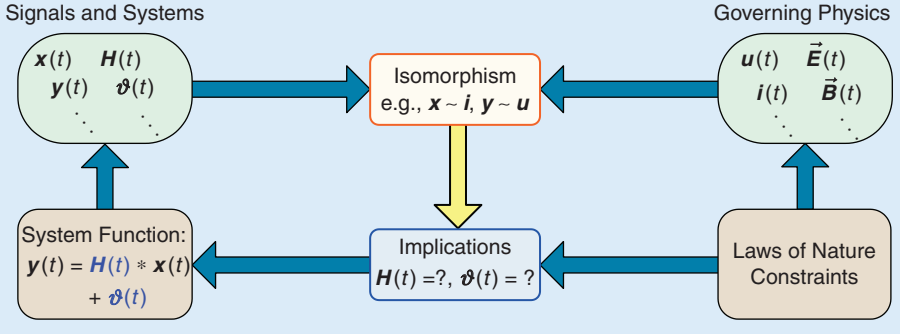

Figure 2. Modeling systems consistently with physics.

The absence of conjugated pairs in information theory and signal processing shows that they are ill equipped to handle fundamental concepts such as energy, power and noise in any way consistent with physics.

unexpected result is perfectly correct and merely a result of the isomorphism (6) and the applicable physical laws represented by Kirchhoff's equations, Ohm's law and the constituent equations of the ideal transformer.

Finally note that $h = 1/2$ corresponds to extracting all available power from the generator (power matching), while $h \to 0$ corresponds to supplying the load with the largest SNR (noise matching). We will meet these two quite different matching strategies again later, for they are essential for optimum implementation of communication systems.

III. The Principles of Multiport Communications

As such simple a circuit as the one shown in Figure 4 leads to rather an involved relationship between the formal symbols of the mathematical model, it is clear that a systematic procedure for extracting all relevant implications is necessary when the situations get more complicated. The multiport communication approach offers such a systematic procedure.

A. Main Assumptions

We consider communication systems which use a sinusoidal carrier to transfer information by modulating its amplitude and/or phase. Such signals are conveniently described by so-called *complex envelopes*. In particular, we define with

$$u_{\mathrm{RF}}(t) = \sqrt{2}\,\mathrm{Re}\{u(t)\,\mathrm{e}^{\mathrm{j}2\pi f_0 t}\} \tag{8}$$

the complex envelope $u(t)$ of a real voltage $u_{\mathrm{RF}}(t)$ which is used for the communication. Herein f_0 denotes the constant frequency of the carrier. Obviously, $u(t)$ contains the amplitude and phase of $u_{\mathrm{RF}}(t)$ in its magnitude and its argument, respectively. The factor $\sqrt{2}$ is included for later convenience.

The complex envelope $i(t)$ of a real current $i_{\mathrm{RF}}(t)$ is defined analogously. In the description of multiports it is convenient to collect all complex port voltage envelopes into a vector $\boldsymbol{u}(t) = [u_1(t)\ \cdots\ u_K(t)]^{\mathrm{T}}$ and all complex port current envelopes into the vector $\boldsymbol{i}(t) = [i_1(t)\ \cdots\ i_K(t)]^{\mathrm{T}}$, where K is the number of ports. In the following, we restrict the discussion to linear (or affine) multiports. With constant complex envelopes, a linear multiport is described by an equation like

$$\boldsymbol{u}(t) = \boldsymbol{Z}(f_0)\,\boldsymbol{i}(t) \tag{9}$$

exactly, where $\boldsymbol{Z}(f_0)$ is the impedance matrix of the multiport evaluated at the carrier frequency. In the following, we will frequently simply write $\boldsymbol{Z}$ meaning $\boldsymbol{Z}(f_0)$. Now the complex envelopes are not constant, but assuming they are sufficiently narrow in bandwidth, (9) holds true in good approximation. Wide-band systems can then be treated as a collection of a number of narrow-band systems each with a slightly different carrier frequency. The total physical power flowing into a multiport being given as the sum of the powers flowing through each port, can be written in complex envelope notation as:

$$P = \mathrm{E}[\mathrm{Re}\{\boldsymbol{u}^{\mathrm{H}}(t)\,\boldsymbol{i}(t)\}] + \mathrm{E}[\mathrm{Re}\{\boldsymbol{u}^{\mathrm{T}}(t)\,\boldsymbol{i}(t)\,\mathrm{e}^{\mathrm{j}4\pi f_0 t}\}]. \tag{10}$$

The expectation operation $\mathrm{E}[\cdot]$ is used to allow the complex envelopes to be random processes rather than deterministic signals. As the second term on the right hand side of (10) can be written $\mathrm{Re}\{\mathrm{tr}(\mathrm{E}[\boldsymbol{i}(t)\,\boldsymbol{i}(t)^{\mathrm{T}}]\boldsymbol{Z}^{\mathrm{T}})\mathrm{e}^{\mathrm{j}4\pi f_0 t}\}$, it follows that

$$\mathrm{E}[\boldsymbol{i}(t)\,\boldsymbol{i}(t)^{\mathrm{T}}] \equiv \mathbf{O} \tag{11}$$

is sufficient to make the expected power be computable as

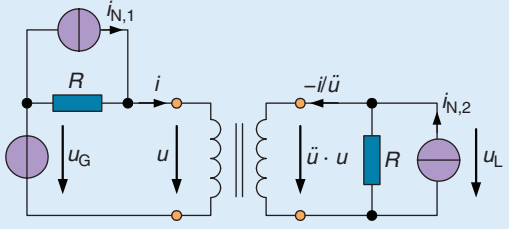

Figure 4. A simple circuit model of a physical communication system.

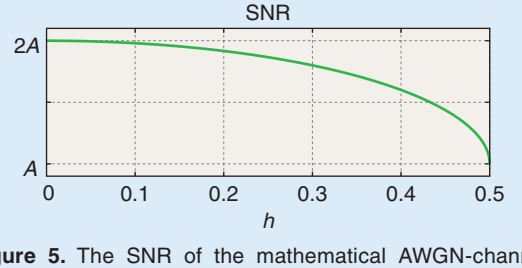

Figure 5. The SNR of the mathematical AWGN-channel model from Figure 3 applied to the circuit model from Figure 4 of an idealized physical communication system using the isomorphism (6). The SNR is shown as a function of the AWGN-channel coefficient h.

$$P = \mathrm{E}[\mathrm{Re}\{\boldsymbol{u}^{\mathrm{H}}(t)\,\boldsymbol{i}(t)\}]. \tag{12}$$

Note that (11) holds true for all linear superpositions of a number of random processes with i.i.d. real- and imaginary parts, especially for complex, circularly symmetric Gaußian random vector processes. If the continuous time complex envelopes are obtained from a discrete-time sequence using *root-Nyquist* pulse shaping [6], and a discrete-time sequence is obtained from the continuous-time signals by matched filtering followed by sampling in symbol time T_s, it can be shown that the power, averaged over a symbol time, can be written as

$$\overline{P} = \mathrm{E}[\mathrm{Re}\{\boldsymbol{u}^{\mathrm{H}}[n]\,\boldsymbol{i}[n]\}], \tag{13}$$

while the multiport is described by:

$$\boldsymbol{u}[n] = \boldsymbol{Z}\boldsymbol{i}[n]. \tag{14}$$

Thus, because of root-Nyquist pulse-shaping, matched filtering and the requirement (11), one can use the same model both for the continuous-time and the discrete-time case. We will, therefore, usually simply write $\boldsymbol{u}$ and $\boldsymbol{i}$, omitting explicit reference to the time index ((t), or $[n]$).

B. Noisy Two-Ports

The affine extension of (9) or (14) obtained by adding to their right hand sides a complex voltage envelope vector $\tilde{\boldsymbol{u}}_{\mathrm{N}}$ which is independent of $\boldsymbol{i}$ and $\boldsymbol{u}$, one obtains a model for a noisy linear multiport. In case there are two ports, one obtains the system shown in Figure 6. Whether the stochastic properties of the noise variables $\tilde{u}_{\mathrm{N},1}$ and $\tilde{u}_{\mathrm{N},2}$ can be inferred from the deterministic properties of the twoport depends on the nature of the noise.

Thermal Equilibrium Noise: In case the twoport internally consists of passive only components and its noise is solely thermal equilibrium noise, the correlation matrix of $\tilde{\boldsymbol{u}}_{\mathrm{N}}$ can be obtained immediately from the impedance matrix of the multiport [12]:

$$\mathrm{E}[\tilde{\boldsymbol{u}}_{\mathrm{N}}\tilde{\boldsymbol{u}}_{\mathrm{N}}^{\mathrm{H}}] = 2\mathrm{k}TW\,(\boldsymbol{Z} + \boldsymbol{Z}^{\mathrm{H}}). \tag{15}$$

Herein, k refers to the Boltzmann constant, while T is the absolute temperature, and W the noise bandwidth of the system ($W = 1/T_s$ for the discrete-time case). This result is a direct consequence of the law of conservation of energy, highlighting again the versatility and importance of the latter. It holds true for any number of ports. In case the multiport is also *reciprocal* ($\boldsymbol{Z} = \boldsymbol{Z}^{\mathrm{T}}$), the noise correlation matrix is proportional to the *real-part* of $\boldsymbol{Z}$. This is, for example, the case for the thermal equilibrium noise of antenna arrays.

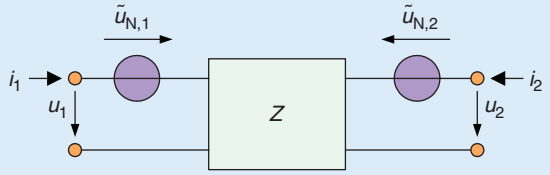

Figure 6. Modeling a noisy twoport as a noiseless twoport and augmenting each port with a noise source.

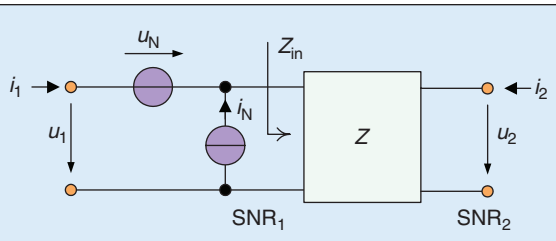

Figure 7. Modeling a noisy twoport as a noiseless twoport and augmenting one port with two noise sources.

Non-Equilibrium Noise: In all the other cases, the stochastic properties of the noise cannot be inferred from the deterministic behavior of the twoport. Instead, all of the physical noise origins inside the twoport have to be modeled by appropriate noise sources. Thus, the twoport cannot be seen as a black-box anymore, but its internal structure has to be known and analyzed. This is, for example, the case for an amplifier twoport. Usually the noise analysis is done by circuit simulation or, better, by measurement.

Under fairly general conditions ($Z_{21} \neq 0$, and $|Z_{11}| < \infty$), the model of a noisy twoport from Figure 6 can be reformulated into the equivalent model shown in Figure 7. It also uses two noise sources: however they are both located at the first port, and one of them is a current source. While both of these noise models are electrically equivalent, the one shown in Figure 7 is much better suited to take part in a multiport model of a communication system. The reason is that the signal to noise ratios at both of its ports are equal ($\mathrm{SNR}_1 \equiv \mathrm{SNR}_2$). From an information theory perspective, it is therefore sufficient to look at the first port. Provided that the stochastic

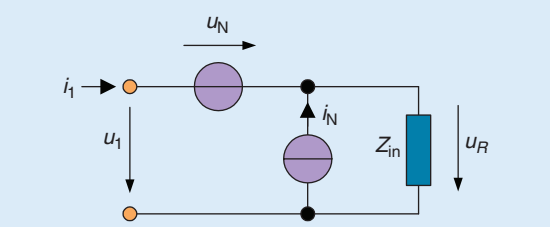

Figure 8. Generic model of a linear noisy receive amplifier.

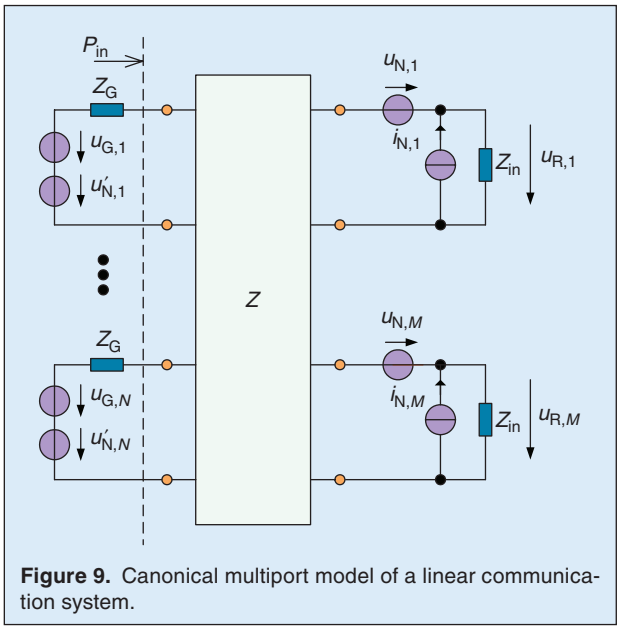

Figure 9. Canonical multiport model of a linear communication system.

properties of the equivalent input noise sources (u_N and i_N) are known, the only further property of the twoport that is of any immediate interest is its input impedance Z_{in}. By interpreting the twoport as a noisy receive amplifier, one therefore obtains the generic model as shown in Figure 8. The port is the input, while the complex envelope u_R of the voltage across Z_{in} constitutes the (SNR-equivalent) output. The *noise parameters* are given by the triple (β, R_N, ρ), defined as

$$\left.\begin{aligned} \beta &= \mathrm{E}\left[|\, i_N|^2\right], \\ R_N &= \sqrt{\mathrm{E}\left[|\, u_N|^2\right]/\mathrm{E}\left[|\, i_N|^2\right]}, \\ \rho &= \mathrm{E}[u_N i_N^*]/\sqrt{\mathrm{E}\left[|\, u_N|^2\right]\cdot \mathrm{E}\left[|\, i_N|^2\right]}. \end{aligned}\right\} \tag{16}$$

The full specification of the amplifier noise, therefore, requires 4 real numbers, at least two of them non-negative.

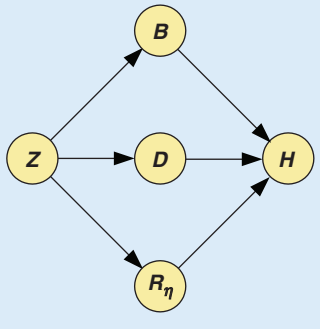

Figure 10. Encapsulation of the physical context into the channel matrix.

C. The Canonical Model

Figure 9 shows a canonical multiport model of a linear multi-input multi-output (MIMO) communication system. The N ports on the left hand side are associated with the N inputs, while the M ports at the right hand side are associated with the outputs of the MIMO system. The transmit signals are obtained from linear generators whose generic model consists of a voltage source with complex envelope $u_{G,n}$ and a series impedance Z_G, where $n \in \{1, 2, \ldots, N\}$. These generators are connected to the N left hand side ports of the linear multiport. The remaining M ports are connected to generic noisy receive amplifier models. The complex envelopes $u_{R,m}$, with $m \in \{1, 2, \ldots, M\}$, constitute the outputs.

At first glance, it appears that the model from Figure 9 is missing M noise sources at its M receive side ports. However, in the canonical model, these receiver side noise sources of the multiport are subsumed in the noise voltage sources $u_{N,m}$ of the receive amplifier. On the other hand, the voltage sources $u'_{N,n}$ at the transmit side ports are made explicit (rather than being subsumed into the $u_{G,n}$), so that $u_{G,n}$ can be used as the sources of the *desired* signal. Of course it is possible to add respective noise sources to the receive side ports for mathematical tractability. Due to their being redundant, they are, however, excluded from the canonical model.

The term *transmit power* is now precisely defined as the power P_{in} which flows through the N transmit side ports with all noise signals switched off:

$$P_{Tx} = P_{in}|_{\text{no noise}}.$$

Expressed in terms of the vector $\boldsymbol{u}_G = [u_{G,1} \cdots u_{G,N}]^T$ of the complex envelopes of the generator's open circuit voltages, the transmit power can be written as

$$P_{Tx} = \frac{1}{4R}\boldsymbol{u}_G^H \boldsymbol{B}\boldsymbol{u}_G. \tag{17}$$

The Hermitian matrix $\boldsymbol{B} \in \mathbb{C}^{N\times N}$ depends on the impedance matrix $\boldsymbol{Z}$ of the multiport, on the values of Z_G and Z_{in} and on the arbitrary reference resistance $R > 0$. The input-output relationship is described by:

$$\boldsymbol{u}_R = \boldsymbol{D}\boldsymbol{u}_G + \sqrt{R}\,\boldsymbol{\eta}, \tag{18}$$

where $\boldsymbol{u}_R = [u_{R,1} \cdots u_{R,M}]^T$ is the vector of the complex envelopes of the received voltages, and the matrix $\boldsymbol{D} \in \mathbb{C}^{M\times N}$ depends on $\boldsymbol{Z}$, Z_G and Z_{in}, while $\boldsymbol{\eta}$ is a vector of the resulting noise complex envelopes. It is usually safe to assume that $\boldsymbol{\eta}$ consists of zero-mean, complex Gaußian distributed random variables such that it is defined by its covariance matrix:

The multiport formalism automatically takes care of all dependencies and makes sure that the relevant physical context is encapsulated into the channel matrix H.

$$\boldsymbol{R}_\eta = \frac{1}{R}\mathrm{E}[\boldsymbol{u}_\mathrm{R}\boldsymbol{u}_\mathrm{R}^\mathrm{H} \mid \boldsymbol{u}_\mathrm{G} = \boldsymbol{0}]. \tag{19}$$

Of course, also $\boldsymbol{R}_\eta$ depends on $\boldsymbol{Z}$, Z_G, Z_in and R, but also on the receiver noise parameters $(\beta, R_\mathrm{N}, \rho)$ and on the stochastic properties of the $\boldsymbol{u}'_{\mathrm{N},n}$.

D. Isomorphism and its Implications

Let $\boldsymbol{x}$ be an N-dimensional vector denoting the N inputs in a channel used in signal processing or information theory. Moreover, let $\boldsymbol{y}$ be an M-dimensional vector denoting the M channel outputs. This model acquires physical meaning by assigning the channel input $\boldsymbol{x}$ to physical quantities at the transmit side, and by assigning the channel output $\boldsymbol{y}$ to some other physical quantities at the receiver side. By such an assignment, an isomorphism is formed between formal symbols and elements from the physical world. Let us try the following isomorphism:

$$\left.\begin{aligned} \boldsymbol{x} &= \frac{1}{2\sqrt{R}}\boldsymbol{B}^{1/2}\boldsymbol{u}_\mathrm{G}, \\ \boldsymbol{y} &= \sqrt{\frac{\sigma^2}{R}}\boldsymbol{R}_\eta^{-1/2}\boldsymbol{u}_\mathrm{R}. \end{aligned}\right\} \tag{20}$$

Herein $\sigma^2 > 0$ is an arbitrary positive number. We assume that both $\boldsymbol{B}$ and $\boldsymbol{R}_\eta$ are invertible matrices. In this way, (20) is bijective, and thus, information preserving. Applying (20) in (18), the following implications are revealed:

1) There is the following input-output relationship:

$$\boldsymbol{y} = \boldsymbol{H}\boldsymbol{x} + \boldsymbol{\vartheta} \tag{21}$$

2) The matrix $\boldsymbol{H} \in \mathbb{C}^{M\times N}$ is given by

$$\boldsymbol{H} = \sqrt{4\sigma^2}\boldsymbol{R}_\eta^{-1/2}\boldsymbol{D}\,\boldsymbol{B}^{-1/2} \tag{22}$$

3) In case that $\boldsymbol{B} > \boldsymbol{0}$, there is

$$\mathrm{E}\left[\|\boldsymbol{x}\|_2^2\right] = P_\mathrm{Tx}, \tag{23}$$

4) and finally,

$$\mathrm{E}[\boldsymbol{\vartheta}\boldsymbol{\vartheta}^\mathrm{H}] = \sigma^2\mathbf{I}_M, \tag{24}$$

where $\mathbf{I}_M$ is the $M\times M$ identity matrix.

With (21), (23) and (24), a standard and easy to use channel model for signal processing or information theory is obtained. The so-called *channel matrix* $\boldsymbol{H}$, defined in (22), contains all the relevant physical context, extracted from the matrices $\boldsymbol{B}$, $\boldsymbol{D}$ and $\boldsymbol{R}_\eta$ of the physical world. As illustrated in Figure 10, each of those three matrices is essentially derived from the same

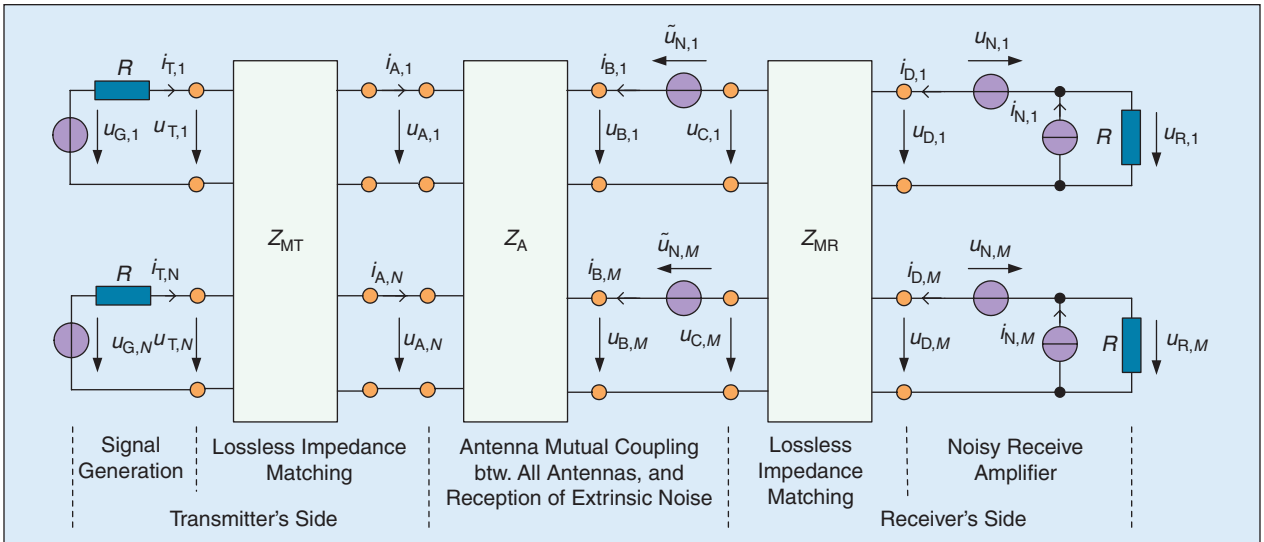

Figure 11. Linear multiport model of a radio multi-antenna communication system covering signal generation, impedance matching, antenna mutual coupling and noise of both extrinsic origin (received by the antennas) and intrinsic origin (from low-noise amplifiers and remaining circuitry).

The reason for a transmit matching multiport is to make the transmit side antennas and the power amplifiers comfortable with each other.

impedance matrix $\boldsymbol{Z}$. This leads to rather complicated dependencies of $\boldsymbol{B}$, $\boldsymbol{D}$ and $\boldsymbol{R}_\eta$ on each other, similar in spirit as (7), only much more involved. The multiport formalism automatically takes care of all dependencies and makes sure that the relevant physical context is encapsulated into the channel matrix $\boldsymbol{H}$.

IV. Wireless Multiport Communication

In the following, we apply the described multiport communication theory to wireless multi-antenna communication systems. In order to facilitate mathematical tractability, the canonical model from Figure 9 is both a little bit expanded and a little bit simplified.

As displayed in Figure 11, the single multiport of the canonical model is split into three multiports: 1. *the antenna multiport*, which encapsulates not only the antennas themselves but also the complete wave propagation between receiver and transmitter, 2. *the transmit matching multiport*, which models all circuitry which is connected between the antenna excitation ports and the power amplifiers of the transmitter, and 3. *the receive matching multiport*, which contains all circuitry which is connected between the receiver's antenna ports and the low-noise amplifiers. The transmit side noise sources from the canonical model are omitted here, because in wireless communications it is usually only the receive side noise that matters. On the other hand, we have explicitly included the antennas' open-circuit noise voltages $\tilde{u}_{\mathrm{N},m}$ because of substantially better mathematical tractability. We note in passing that a similar multiport model was also used in [13], albeit missing consistent treatment of noise.

A. Transmit Matching

The reason for a transmit matching multiport is to make the transmit side antennas and the power amplifiers comfortable with each other. In practice, this usually means that the multiport impedance presented by the transmit antennas is changed by the transmit matching multiport in such a way which allows all the available power to be extracted from the amplifiers. This strategy is called *power matching*. If the matching multiport is lossless, the amplifier's available power is fed into the antenna array. If the latter is lossless, too, the available power is completely radiated. As the impedances of the power amplifiers in Figure 11 are uncoupled and equal to R, a *lossless* transmit matching multiport, set up for power matching, will present to the power amplifiers a bank of uncoupled resistances of the same value R. In the following, we assume that such a lossless matching multiport is employed.

B. Receive Matching

While extracting and radiating maximum power is clearly a sensible goal for the transmitter, the extraction of maximum power from the electromagnetic field by the receiver is usually sub-optimum. Instead, the receiver should try to obtain the largest possible signal to noise ratio (SNR) at the outputs of its low noise amplifiers. A matching strategy which aims at maximization of SNR is called *noise matching* [14], [15]. If the receive matching multiport is lossless, it can provide this maximization without adding noise of its own, and without dissipating desired signal energy. In the following, we assume that such a lossless matching multiport is employed.

C. Antenna Noise

The open-circuit noise voltage which appears at the antenna ports comes from two effects: 1. from received background radiation, and 2. from fluctuations caused by its own heat loss. Lossless antennas only have noise from background radiation. In case that the antennas are in thermal equilibrium with their environment, the covariance matrix of the complex envelopes of their open-circuit noise voltages is proportional to the real-part of their impedance matrix [12]. In the following, we assume that this is the case.

D. Antenna Multiport

The antenna multiport is responsible to model: 1. the interaction of the transmit side antennas with themselves due to electromagnetic mutual near-field coupling, 2. the interaction of the receive side antennas with themselves due to electromagnetic mutual near-field coupling, and 3. the interaction of the transmit array and the receive array due to electromagnetic mutual far-field coupling. The latter critically depends on the wave propagation environment, while the first and second depend mostly on the geometry of the arrays and the type and orientation of the antennas. In some simple cases, the impedance matrix $\boldsymbol{Z}_\mathrm{A}$ of the antenna multiport may be calculated analytically. In more realistic situations, a full-wave solution of Maxwell's equations is necessary, which can only be done numerically. At any rate, the result of all antenna interaction is captured in the impedance matrix $\boldsymbol{Z}_\mathrm{A}$, which we can partition into four blocks:

$$\boldsymbol{Z}_{\mathrm{A}} = \begin{bmatrix} \boldsymbol{Z}_{\mathrm{AT}} & \boldsymbol{Z}_{\mathrm{ATR}} \\ \boldsymbol{Z}_{\mathrm{ART}} & \boldsymbol{Z}_{\mathrm{AR}} \end{bmatrix}. \tag{25}$$

Herein, $\boldsymbol{Z}_{\mathrm{AT}} \in \mathbb{C}^{N\times N} \cdot \Omega$ is the transmit impedance matrix. It describes the interaction of the transmit side antennas for the case of vanishing port currents at the receive side. Similarly, $\boldsymbol{Z}_{\mathrm{AR}} \in \mathbb{C}^{M\times M} \cdot \Omega$ is the receive impedance matrix. It describes the interaction of the receive side antennas for the case of vanishing port currents at the transmit side. Finally, $\boldsymbol{Z}_{\mathrm{ART}}$ models the action of the transmit array on the receive array, while $\boldsymbol{Z}_{\mathrm{ATR}}$ models the action of the receive array back on the transmit array. Because antennas are reciprocal, these two actions are the same, and $\boldsymbol{Z}_{\mathrm{ATR}} = \boldsymbol{Z}_{\mathrm{ART}}^{\mathrm{T}}$. We note in passing, that from this circuit theoretic description, it is also possible to arrive at a more abstract description of antenna mutual coupling which is based on a special kind of non-Euclidean geometry [16].

E. The Channel Matrix

For the system from Figure 11, together with the assumptions in Sections IV-A, IV-B, IV-C and IV-D, one can compute the $\boldsymbol{B}$, $\boldsymbol{D}$ and $\boldsymbol{R}_{\eta}$ matrices, and from them, using (22), the channel matrix $\boldsymbol{H}$. By setting

$$\sigma^2 = 4\mathrm{k}TW\mathrm{NF}_{\mathrm{min}}, \tag{26}$$

where $\mathrm{NF}_{\mathrm{min}}$ is the minimum noise figure [17]–[20] of the low noise amplifiers which results from noise matching, one finds the surprisingly simple expression [19]–[20]:

$$\boldsymbol{H} = (\mathrm{Re}\{\boldsymbol{Z}_{\mathrm{AR}}\})^{-1/2}\boldsymbol{Z}_{\mathrm{ART}}(\mathrm{Re}\{\boldsymbol{Z}_{\mathrm{AT}}\})^{-1/2}. \tag{27}$$

Recall that the matrices $\boldsymbol{Z}_{\mathrm{AR}}$ and $\boldsymbol{Z}_{\mathrm{AT}}$ quantify the antenna mutual coupling *within* the receive-and transmit-side arrays (*intra-array coupling*), while $\boldsymbol{Z}_{\mathrm{ART}}$ quantifies the antenna mutual coupling *between* receive- and transmit-side arrays (*inter-array coupling*). It turns out that the key difference between the results obtained with the help of multiport communication and those obtained with the help of standard array signal processing comes from the fact that the latter ignores mutual coupling *within* the arrays. That is, standard array signal processing emerges as a limiting case of multiport communication, when $\boldsymbol{Z}_{\mathrm{AR}}$ and $\boldsymbol{Z}_{\mathrm{AT}}$ become scaled identity matrices. In many practical situations however, fundamental principles of physics prevent those matrices from becoming scaled identities. The very existence of the inverse square root of their real-parts in (27), is then responsible for a host of interesting effects. But before we can have a look into some of those, we first have to obtain some information about the nature of those matrices.

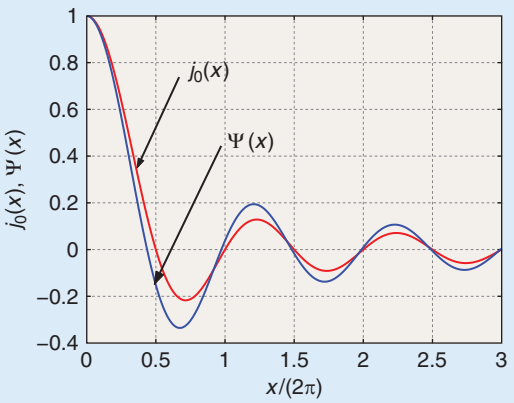

Figure 12. Comparison of the coupling function for Hertzian dipoles ($\Psi(x)$) and for hypothetical isotrops ($\mathrm{j}_0(x)$).

F. Intra-Array Coupling

Because the antennas of an antenna array are usually located in rather close proximity to each other, the intra-array coupling is due to the antennas responding to the near-fields generated by their neighbors and by themselves. From (27) it is however clear that we do not need to know the whole near-field coupling to come up with the channel matrix. Knowing the real-part of the transmit/receive impedance matrix is already enough.

Consider an antenna array in otherwise empty space. For antennas are reciprocal, the physical power which flows into the antenna array is given by:

$$P_{\mathrm{in}} = \mathrm{E}[\boldsymbol{i}^{\mathrm{H}}\mathrm{Re}\{\boldsymbol{Z}_{\mathrm{AT}}\}\boldsymbol{i}].$$

If the antennas are lossless (i.e., have no heat loss), the law of conservation of energy demands that the power P_{in} is radiated out in space. Now the radiated power can also be computed from integrating the Poynting vector over any closed surface that contains the whole antenna array [21]. Making this surface large enough, the integration can be carried out entirely in the *far-field* of the array. Thus, despite the intra-array coupling being a near-field effect, one can obtain important information about it, namely the $\mathrm{Re}\{\boldsymbol{Z}_{\mathrm{AT}}\}$, from *far-field* considerations and the law of conservation of energy. This is yet another example of how conservation laws can help solve an otherwise complicated problem. Following this approach, for an array of Hertzian dipoles uniformly placed on a line which is perpendicular to all dipoles, it is shown in [22] that:

$$\mathrm{Re}\{\boldsymbol{Z}_{\mathrm{AT}}\} = R_{\mathrm{r,HD}}\boldsymbol{C}_{\mathrm{HD}}, \text{ where } (\boldsymbol{C}_{\mathrm{HD}})_{m,n} = \Psi(kd|m-n|), \tag{28}$$

d being the inter-element spacing, and

Any mathematical system model can be made consistent with the governing physics by following a two-step procedure.

$$\Psi(x) = \frac{3}{2}\left(\frac{\sin x}{x} + \frac{\cos x}{x^2} - \frac{\sin x}{x^3}\right), \tag{29}$$

where $k = 2\pi/\lambda$, with λ as the wavelength, and $R_{\mathrm{r,HD}} > 0$ is the radiation resistance (see, e.g., [23]) of the Hertzian dipole. The same coupling function (29) can also be obtained from near-field considerations [24]. Note that $\boldsymbol{C}_{\mathrm{HD}}$ has unity entries on its main diagonal. For small element spacing (with respect to the wavelength), the off-diagonal components are also large in magnitude. For example, setting $d = \lambda/3$, one finds for a 3-element array that

$$\boldsymbol{C}_{\mathrm{HD}} = \begin{bmatrix} 1 & 0.31 & -0.34 \\ 0.31 & 1 & 0.31 \\ -0.34 & 0.31 & 1 \end{bmatrix},$$

which is far from being a scaled identity. In the same way as for the Hertzian dipoles one can also calculate the mutual coupling of isotropic radiators, by merely replacing the direction dependence of the Hertzian dipole by a constant [22]. Even though Maxwell's equations do not permit a coherent isotropic radiation, one can, in this way, obtain the coupling matrix $\boldsymbol{C}$ of a uniform linear array of *hypothetical* isotropic radiators:

$$(\boldsymbol{C})_{m,n} = \mathrm{j}_0(kd|n-m|), \quad \text{where } \mathrm{j}_0(x) = \frac{\sin x}{x}, \tag{30}$$

so that

$$\mathrm{Re}\{\boldsymbol{Z}_{\mathrm{AT}}\} = R_{\mathrm{r}}\boldsymbol{C}, \tag{31}$$

with some constant $R_{\mathrm{r}} > 0$. The main difference to the case of Hertzian dipoles is, therefore, that the coupling function $\mathrm{j}_0(\cdot)$ is used instead of $\Psi(\cdot)$. At first glance, $\mathrm{j}_0(x)$ and $\Psi(x)$ appear to be rather different. However, when we look at Figure 12, we observe that there actually is a striking similarity. Both functions are decreasing at first, when x is increased from zero, and then display an oscillatory behavior as x is further increased. While $\mathrm{j}_0(x)$ has equidistant roots (integer multiples of π), the function Ψ has *almost* equidistant roots at *almost* the same positions as $\mathrm{j}_0(x)$. From what we see in Figure 12, we may therefore conclude that $\mathrm{j}_0(x)$, and $\Psi(x)$ are *qualitatively the same*. This justifies the use of isotropic radiators in the theoretical treatment of antenna arrays, even though they are not permitted by Maxwell's theory. The obtained results for isotropic radiators are qualitatively the same as the ones obtained for Hertzian dipoles. The differences are, therefore, only quantitative and turn out to be not too large [22]. Since arrays of isotrops are determined solely by the collection of the mutual distances, one can easily generalize the coupling matrix for arbitrary arrays of isotrops:

$$(\boldsymbol{C})_{m,n} = \mathrm{j}_0(kd_{m,n}), \tag{32}$$

where $d_{m,n} = d_{n,m}$ is the geometrical distance between the m-th and the n-th isotrop. The presence of a medium (rather than air or vacuum) can be taken care of by using the wavelength suitable for the medium when computing $k = 2\pi/\lambda$.

Because one can use the same antenna array for reception as for transmission, the matrix $\mathrm{Re}\{\boldsymbol{Z}_{\mathrm{AR}}\}$ is calculated exactly the same as $\mathrm{Re}\{\boldsymbol{Z}_{\mathrm{AT}}\}$.

G. Inter-Array Coupling

The inter-array coupling obviously depends on the wave propagation environment present between transmitter and receiver, the simplest case being empty space. If the separation is large, the coupling reduces inversely with distance. Furthermore, the same phase must occur in integer multiples of the wavelength. Assuming isotropic radiators, we do not have to worry about directional or orientational dependence. Hence,

$$(\boldsymbol{Z}_{\mathrm{ART}})_{m,n} = \Gamma_0 \frac{\mathrm{e}^{-\mathrm{j}kr_{m,n}}}{r_{m,n}}, \tag{33}$$

where Γ_0 is a constant, and $r_{m,n}$ is the geometric distance between the m-th antenna of the receiver and the n-th antenna of the transmitter.

Note that (33) requires the concept of *canonical minimum scattering* (CMS) antennas [25]. A CMS antenna becomes essentially »invisible« if the current at its excitation port vanishes. For other antennas in its neighborhood, it is then as if the CMS antenna with zero port

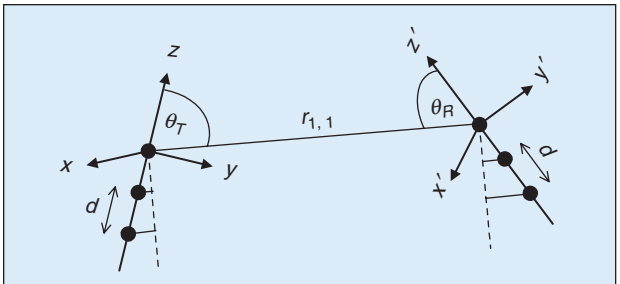

Figure 13. Two arbitrarily oriented uniform linear arrays in free space.

current were not present physically. While the CMS property is an idealization of reality, a half-wavelength dipole (or shorter) made of *thin* wire is a good approximation [26]. We prescribe this ideal behavior also to the hypothetical isotropic radiator.

The best way to describe arrays of CMS antennas is via the *impedance matrix* description, for an element of $\boldsymbol{Z}$ is obtained by letting all port currents, except one, become zero. Together with the CMS property, the problem is therefore reduced to *pairs* of antennas. In (33) one can, therefore, *not* use, say, the admittance matrix or scattering matrix, for these would imply non-vanishing port currents, prohibiting pair-wise treatment. One would have to consider the fields due to non-vanishing port currents of all antennas and not only the field generated by the n-th transmit side antenna. Obviously, this is much more complicated and better avoided by use of the impedance matrix, the canonical way to describe CMS antennas.

Picking up development by defining $r_{m,n} = r_{1,1} + \Delta r_{m,n}$, we can re-write the right hand side of (33) in the following way: $\alpha \mathrm{e}^{-\mathrm{j}k\Delta r_{m,n}} r_{1,1}/r_{m,n}$, with $\alpha = \Gamma_0 \mathrm{e}^{-\mathrm{j}kr_{1,1}}/r_{1,1}$. For the case of two uniform linear arrays, as shown in Figure 13, there is

$$\Delta r_{m,n} = d(n-1)\cos(\theta_\mathrm{T}) + d(m-1)\cos(\theta_\mathrm{R}).$$

Moreover, one can replace the term $r_{1,1}/r_{m,n}$ by unity, because receiver and transmitter are usually separated much farther than the distances of the antennas inside the arrays. Thus, (33) becomes for the case of uniform linear arrays:

$$\boldsymbol{Z}_\mathrm{ART} = \alpha \boldsymbol{a}_\mathrm{R}(\theta_\mathrm{R})\boldsymbol{a}_\mathrm{T}^\mathrm{T}(\theta_\mathrm{T}), \tag{34}$$

where

$$\boldsymbol{a}_\mathrm{T}(\theta) = [1 \;\; \mathrm{e}^{-\mathrm{j}kd\cos\theta} \;\; \mathrm{e}^{-2\mathrm{j}kd\cos\theta} \;\; \cdots \;\; \mathrm{e}^{-(N-1)\mathrm{j}kd\cos\theta}]^\mathrm{T},$$
$$\boldsymbol{a}_\mathrm{R}(\theta) = [1 \;\; \mathrm{e}^{-\mathrm{j}kd\cos\theta} \;\; \mathrm{e}^{-2\mathrm{j}kd\cos\theta} \;\; \cdots \;\; \mathrm{e}^{-(M-1)\mathrm{j}kd\cos\theta}]^\mathrm{T},$$

are the so-called transmit and receive *steering vectors*. Multipath propagation is then easily introduced by

$$\boldsymbol{Z}_\mathrm{ART} = \sum_i \alpha_i \boldsymbol{a}_\mathrm{R}(\theta_{\mathrm{R},i})\boldsymbol{a}_\mathrm{T}^\mathrm{T}(\theta_{\mathrm{T},i}).$$

A stochastic model for fading propagation conditions arises by letting the α_i be random variables. Assuming $\mathrm{E}[\alpha_i \alpha_j^*] = \gamma_i \delta_{i,j}$, with $\delta_{i,j}$ being unity for $i = j$ and zero else, one obtains the correlation matrices:

$$\mathrm{E}[\boldsymbol{Z}_\mathrm{ART}\boldsymbol{Z}_\mathrm{ART}^\mathrm{H}] = N\sum_i \gamma_i \boldsymbol{a}_\mathrm{R}(\theta_{\mathrm{R},i})\boldsymbol{a}_\mathrm{R}^\mathrm{H}(\theta_{\mathrm{R},i}), \tag{35}$$

$$\mathrm{E}[\boldsymbol{Z}_\mathrm{ART}^\mathrm{H}\boldsymbol{Z}_\mathrm{ART}] = M\sum_i \gamma_i \boldsymbol{a}_\mathrm{T}^*(\theta_{\mathrm{T},i})\boldsymbol{a}_\mathrm{T}^\mathrm{T}(\theta_{\mathrm{T},i}). \tag{35a}$$

The $\gamma_i \geq 0$ are proportional to the average power gain of the i-th path of the multipath propagation environment. By choosing a (large) number of directions $(\theta_{\mathrm{T},i}, \theta_{\mathrm{R},i})$, and assigning appropriate values to the γ_i, one can realize fading multipath propagation with arbitrary angle-spreads. We note in passing that the interface to common spatial channel models (SCM), e.g., to [27] for 3Gpp-UMTS, works such that what those SCM refer to as »channel-coefficients« should be interpreted as the elements of $\boldsymbol{Z}_\mathrm{ART}$, instead of $\boldsymbol{H}$.

V. Applications

Let us now apply the described multiport communication theory of wireless multi-antenna systems to several interesting figures of merit of such systems. In the present view, the multiple antennas can be used to different benefit compared to systems which have only a single antenna at either side of the link: 1. Reduction of necessary transmit power. This benefit is quantified by the *array gain* [19]. 2. Reduction of the variation of the channel quality. A suitable figure of merit is the *diversity measure* [28]. 3. Increase of the data rate by spatial multiplexing [29]. This is best analyzed in terms of mutual information, or channel capacity of the individual streams. 4. Increase of the capacity region in a multi-user context [30]. We focus here on the multiple-access scenario, where one receiver listens to several users who transmit simultaneously.

A. Array Gain

Consider a wireless multi-antenna communication system with N transmit antennas and M receive antennas. As described in Section III-D, such a system can be modeled as a multi-input multi-output (MIMO) system described by

$$\boldsymbol{y} = \boldsymbol{H}\boldsymbol{x} + \boldsymbol{\vartheta}, \quad P_\mathrm{Tx} = \mathrm{E}[\|\boldsymbol{x}\|_2^2], \quad \mathrm{E}[\boldsymbol{\vartheta}\boldsymbol{\vartheta}^\mathrm{H}] = \sigma^2\mathbf{I}.$$

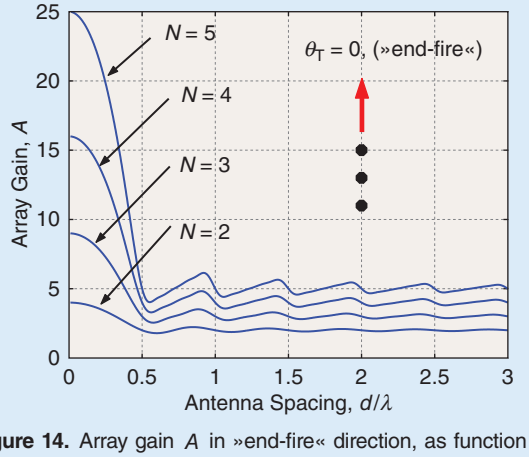

Figure 14. Array gain A in »end-fire« direction, as function of the antenna separation for different number N of antennas.

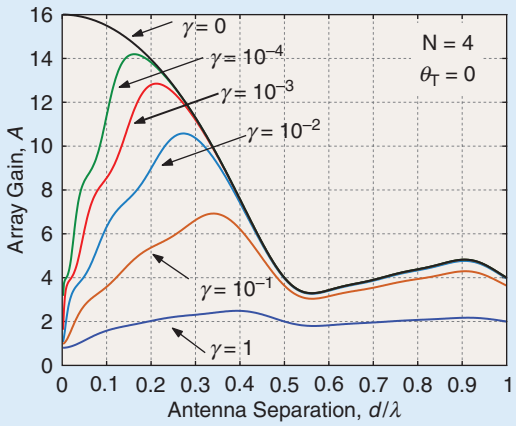

Figure 15. Array gain of a uniform linear array of $N = 4$ lossy isotrops, when beamforming in »end fire« direction is applied.

Every MIMO system of this kind can be turned into a virtual single-input single-output (SISO) system by virtue of transmit and receive beamforming:

$$\boldsymbol{x} = \boldsymbol{t} \cdot s, \quad \hat{s} = \boldsymbol{r}^{\mathrm{H}} \boldsymbol{y},$$

where s and $\hat{s}$ are the transmit and receive signals of the virtual SISO system, and $\boldsymbol{t} \in \mathbb{C}^{N\times 1}$ and $\boldsymbol{r} \in \mathbb{C}^{M\times 1}$ are the transmit and receive beamforming vectors. The SNR w.r.t. $\hat{s}$ is given by

$$\mathrm{SNR} = \frac{P_{\mathrm{Tx}}}{\sigma^2} \frac{|\boldsymbol{r}^{\mathrm{H}} \boldsymbol{H} \boldsymbol{t}|^2}{\|\boldsymbol{r}\|_2^2 \|\boldsymbol{t}\|_2^2}.$$

The array gain is defined as [19]:

$$A = \frac{\max \mathrm{SNR}}{\max \mathrm{SNR}|_{M=N=1}}\Big|_{P_{\mathrm{Tx}}/\sigma^2 = \mathrm{const}}, \tag{36}$$

where the maximization in the numerator is done with respect to $\boldsymbol{r}$ and $\boldsymbol{t}$, while in the denominator it is with respect to the choice of which of the N transmit and which of the M receive antennas to use. Therefore, the array gain quantifies the maximum increase in SNR of the virtual SISO systems, which comes by using all N antennas at the transmitter and all M antennas at the receiver simultaneously, compared to the case where transmitter and receiver use only a single antenna each. The array gain can then be computed as:

$$A = \frac{\max \mathrm{EigVal}\{\boldsymbol{H}\boldsymbol{H}^{\mathrm{H}}\}}{\max |\boldsymbol{H}|_{M=N=1}|^2}. \tag{37}$$

Of course, the matrix $\boldsymbol{H}$ in the denominator is a scalar! Note that $\boldsymbol{H}^{\mathrm{H}}\boldsymbol{H}$ can be substituted for $\boldsymbol{H}\boldsymbol{H}^{\mathrm{H}}$ in case that it yields the smaller matrix, for they have the same non-zero eigenvalues. As a corollary: if $\boldsymbol{H}$ is a vector (single row, or single column), then the numerator equals its squared Euclidean norm. Such a case refers to either single-input multi-output (SIMO) or multi-input single-output (MISO) systems. In either case, the array gain is easy to compute.

Considering a system which employs multiple antennas at the transmitter only, and assuming a uniform linear array of isotrops, using (34) and (31) in (27), the array gain from (37) becomes $A = \boldsymbol{a}_{\mathrm{T}}^{\mathrm{H}}(\theta_{\mathrm{T}})\boldsymbol{C}^{-1}\boldsymbol{a}_{\mathrm{T}}(\theta_{\mathrm{T}})$. Because $\|\boldsymbol{a}_{\mathrm{T}}(\theta_{\mathrm{T}})\|_2^2 = N$, it follows for the array gain of a uniform linear array of isotrops:

$$A = N\frac{\boldsymbol{a}_{\mathrm{T}}^{\mathrm{H}}(\theta_{\mathrm{T}})\boldsymbol{C}^{-1}\boldsymbol{a}_{\mathrm{T}}(\theta_{\mathrm{T}})}{\|\boldsymbol{a}_{\mathrm{T}}(\theta_{\mathrm{T}})\|_2^2}. \tag{38}$$

It depends not only on N, but also on the dedicated direction θ_{T} of beamforming, and also on the antenna spacing, d, which influences both $\boldsymbol{a}_{\mathrm{T}}(\theta_{\mathrm{T}})$ and $\boldsymbol{C}$. Only if $\boldsymbol{C}$ is the identity matrix, the array gain is independent of θ_{T} and equals the number N of antennas. However, $\boldsymbol{C}$ is only an identity if d is an integer multiple of half the wavelength, as can be seen from (30). Thus, all other antenna spacings result in an array gain which depends on the dedicated direction of beamforming, and whose value is usually different from N, where both larger and smaller values are possible. For $\theta_{\mathrm{T}} = 0$, the so-called »end-fire« direction, the resulting array gain is shown in Figure 14. For large antenna spacings, the array gain is more or less equal to the number of antennas. However, as soon as the distance d drops below half of a wavelength, there is sharp increase of array gain with decreasing d which approaches the *square* of the number of antennas as d/λ approaches zero.

Interestingly, the effect of a quadratic growth of array gain with antenna number was already predicted in [31] as early as 1946, and was surely known, yet not spelled out, by the author of [32] three years earlier. However, such »super-gain« effects do not seem to have been very well received, perhaps because of the work [33], which unveiled the high sensitivity of super-gain arrays with respect to the presence of heat loss in the antennas. In practice, heat loss would actually eat up all the super-gain. Until recently, the term super-gain was therefore described as a »miss-nomer« in standard textbooks [23], [34]. However, it was shown theoretically in [35] and by experiment in [36], that large amounts of super-gain can be retained even with lossy antennas, provided the antenna spacing is chosen properly. To see this, we can adopt a simple model for antenna heat loss by using

$$\mathrm{Re}\{\boldsymbol{Z}_{\mathrm{AT}}\} = R_{\mathrm{r}}\boldsymbol{C} + R_{\mathrm{d}}\mathbf{I},$$

where R_{d} is the effective dissipation resistance of the antennas. Thus, all one has to do to arrive at the array gain of a uniform linear array of *lossy* isotrops, is to

replace in (38) the coupling matrix $\boldsymbol{C}$ by $\boldsymbol{C}+\gamma\mathbf{I}$, where $\gamma = R_{\rm d}/R_{\rm r}$ is the loss-factor.

The results for the case of $N = 4$ isotrops is shown in Figure 15. Cleary, the situation is not that bad. Having a $\gamma = 0.01$, and choosing the optimum separation of $d = 0.27\lambda$, the array gain is still by 4.2 dB larger than the number of isotrops in the array, and 1.8 dB away from the theoretical maximum for lossless isotrops. Even a $\gamma = 0.1$ allows for having super-gain in end-fire direction (gain of 7 with four elements) by placing the isotrops by $\lambda/3$ apart. However, the sensitivity to the presence of heat loss increases with antenna number. As a consequence, the quadratic growth of array gain with antenna number eventually has to yield to an almost linear growth for larger numbers of lossy isotrops [35]. Between two and four antennas per dimension seems to be the practical range. Such numbers are interesting for many mobile communication devices.

B. Diversity

When electromagnetic waves hit an object they shake up the object's free electrons (if any). These accelerated electrons generate electromagnetic waves of their own which superimpose on the incident waves. Because of the Doppler effect, the presence of relative mobility causes each new wave to have a slightly different frequency. Consequently, their superposition results in a time-varying signal strength at a receive antenna, which shows the characteristic occasional deep fades resulting from a destructive superposition. A common attempt to lower the chance of falling into a deep fading hole is to employ *antenna diversity*, which combines signals from several antennas. If the antennas are spaced sufficiently far apart, chances are that the respective signal amplitudes will be (almost) uncorrelated and *simultaneous* deep fades become much less likely, thereby improving link reliability [37].

The correlation between antenna signals essentially depends on a number of factors. Two prominent ones are the angular power density and the antenna separation [38]. In general, receiving substantial amount of power from a wide range of angles tends to make for low correlation, as does a large separation of antennas, preferably by several wavelengths [39]. Close antenna spacing is therefore traditionally avoided in diversity applications because it is feared that the closely spaced antennas will receive almost the same signal, thus rendering antenna diversity ineffective. This however ignores another important factor: the antenna mutual coupling. It turns out that mutual coupling not only has important impact on array gain (as we have seen before), but also affects the diversity performance in a remarkable way.

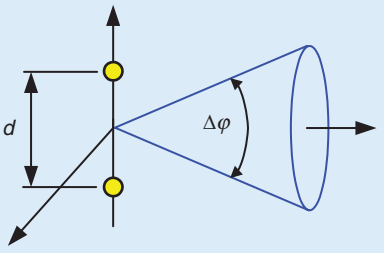

Figure 16. Two isotrops in multipath propagation environment with conic angle-spread around front-fire direction.

A simple way to quantify how well a diversity system performs is to consult the so-called *diversity measure* [28]. To this end, consider a SIMO system described by

$$\boldsymbol{y} = \boldsymbol{h}s + \boldsymbol{\vartheta}, \quad \mathrm{E}[\boldsymbol{\vartheta}\boldsymbol{\vartheta}^{\rm H}] = \sigma^2\mathbf{I},$$

which is used to model a multi-antenna system with multiple antennas at the receiver. The vector $\boldsymbol{y}$, thus, contains M noisy »copies« of a signal s, received over different diversity branches. Diversity combining of all signals yields the signal $\hat{s} = \boldsymbol{w}^{\rm H}\boldsymbol{y}$, where the combining vector $\boldsymbol{w} \in \mathbb{C}^{M\times 1}$ can be chosen to maximize the SNR, which yields the value of $(\sigma_s^2/\sigma^2)\|\boldsymbol{h}\|_2^2$, where $\sigma_s^2 = \mathrm{E}[|s|^2]$. The diversity measure is then given by:

$$D = \frac{(\mathrm{E}[\mathrm{SNR}])^2}{\mathrm{Var}[\mathrm{SNR}]} = \frac{(\mathrm{Tr}\,\mathrm{E}[\boldsymbol{h}\boldsymbol{h}^{\rm H}])^2}{\mathrm{Tr}(\mathrm{E}[\boldsymbol{h}\boldsymbol{h}^{\rm H}])^2},$$

where the last equality assumes the components of the channel vector $\boldsymbol{h}$ to be complex, circularly symmetric Gaußian distributed, i.e., a Rayleigh fading channel. The symbol Tr refers to the matrix trace, i.e., to the sum of its diagonal components. The diversity measure is the inverse of the relative fluctuation of the SNR. The larger

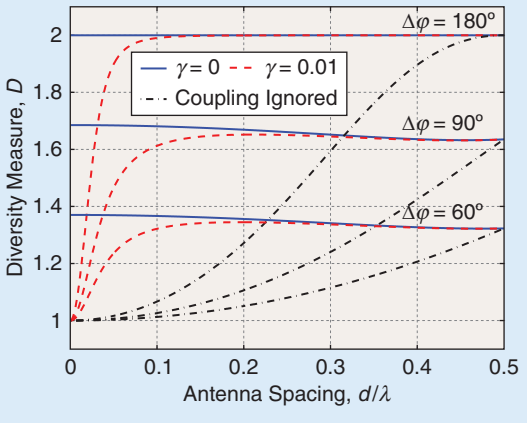

Figure 17. Diversity measure for the system from Figure 16.

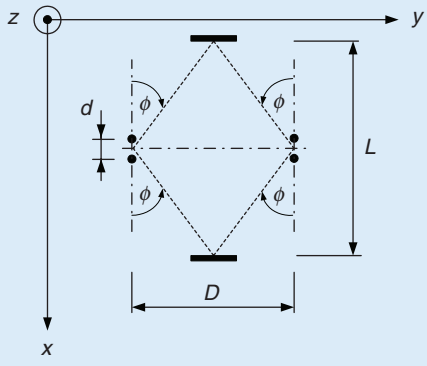

Figure 18. Top-view of a test system for multistreaming with compact arrays.

it is, the less the SNR fluctuates with respect to its mean value, and the better is the performance of the diversity combing. This is the idea of the diversity measure. Due to $\boldsymbol{h}$ being Gaußian distributed, it holds true that $1 \le D \le M$, such that optimum diversity performance is characterized by having $D = M$. Using (27) with $\boldsymbol{h}$ in place of $\boldsymbol{H}$, and assuming isotropic radiators by virtue of (31), one obtains:

$$\mathrm{E}[\boldsymbol{h}\boldsymbol{h}^{\mathrm{H}}] = \mathrm{const} \cdot \boldsymbol{C}^{-1/2}\mathrm{E}[\boldsymbol{Z}_{\mathrm{ART}}\boldsymbol{Z}_{\mathrm{ART}}^{\mathrm{H}}]\,\boldsymbol{C}^{-1/2}.$$

Using (35), the matrix $\mathrm{E}[\boldsymbol{Z}_{\mathrm{ART}}\boldsymbol{Z}_{\mathrm{ART}}^{\mathrm{H}}]$ can be found for any given angular power distribution. Figure 16 shows, for the case of $M = 2$, an angular power distribution which is uniform inside a cone of opening angle $\Delta\varphi$ and centered around the so-called front-fire direction, i.e., perpendicular to the array axis. It can be shown (see [40]), that in this case

$$\mathrm{E}[\boldsymbol{Z}_{\mathrm{ART}}\boldsymbol{Z}_{\mathrm{ART}}^{\mathrm{H}}] = \mathrm{const}\begin{bmatrix} 1 & \rho_{\mathrm{S}} \\ \rho_{\mathrm{S}} & 1 \end{bmatrix},$$

where

$$\rho_{\mathrm{S}} = \frac{\int_0^{\Delta\varphi/2} \mathrm{J}_0(kd\sin\tau)\sin(\tau)\,\mathrm{d}\tau}{2\sin^2(\Delta\varphi/4)},$$

and $\mathrm{J}_0(\cdot)$ is the Bessel function of the first kind and zero-th order. The integral must be solved numerically.

The diversity measure for this scenario is displayed in Figure 17. The three solid curves correspond to the case of lossless isotrops. As can be seen, the diversity performance is almost unaffected by the antenna spacing d, but essentially only depends on the amount of angle-spread. For an opening angle of 180° the maximum diversity is achieved at *any* antenna separation. Thus, *contrary to common belief, antenna separation is not a fundamental limit to the diversity performance.*

The three dashed curves in Figure 17 correspond to the case of lossy isotrops, with loss factor (see last part of Section V-A) of $\gamma = 0.01$. For $d > \lambda/4$, this loss has essentially no impact, but for decreasing antenna spacing, the diversity measure drops monotonically and reaches its minimum as d/λ approaches zero. *For small antenna separation, it is heat-loss which, ultimately, limits the diversity performance.* For $\Delta\varphi = 180^{\circ}$ and loss factor of $\gamma = 0.01$ one can nevertheless maintain $D \ge 1.5$ for separations down to 1/40 of a wavelength! Despite heat loss, the diversity performance of compact arrays can be excellent. Interestingly, compact diversity arrays have been built and proposed for mobile devices already a decade ago [41]. Their theoretical justification was given later in [40].

The three dash-dotted curves in Figure 17 correspond to the case where the antenna mutual coupling is simply *ignored.* It reflects the still wide-spread belief that one cannot have good diversity performance with small separations. It is plain to see from Figure 17 how far this is from the truth and how important both the antenna mutual coupling and its consistent modeling really is.

C. Multistreaming

Besides being able to provide array gain and diversity, MIMO systems potentially support the transfer of several data streams at the same time using the same band of frequencies. In order for this so-called *multistreaming* to work, the channel matrix must have at least two relatively large singular values. Spatial signal processing at the transmit and the receive side can then be used to establish at least two independent communication channels [29].

When modeling a wireless multi-antenna communication system as a MIMO system, an interesting question arises: what kind of *physical* structure should the propagation channel have so that multistreaming is well supported? The simple answer is that it must have a structure which leads to a channel matrix with many strong singular values. But what is this structure? Experience shows that it can help when there are many scattering objects located between receiver and transmitter, which lead to a rich multipath propagation environment. Such an environment is, however, not strictly necessary. Even in a free-space (line of sight) propagation environment, that is, in total absence of any scatterers, multistreaming may be supported, provided the antenna positions are carefully selected and the array sizes are similar to the distance between receiver and transmitter [42]. The latter qualification is a serious restriction but can be rather easily fulfilled for satellite communications with far-separated ground stations.

Another important question is how to couple to this environment, that is, what kind of and how many antennas should be used and how should they be arranged in space, so that multistreaming is well supported? This

question, too, is difficult to answer. Experience tells us that it may help if the antennas are not too selective in direction and their separation inside their arrays is pretty large, at least half of the wavelength [30]. Yet again, it turns out that it is *not* strictly necessary to have any large antenna separations. In fact, it is possible to obtain good multistreaming capability even with very compact antenna arrays. In order to explore a little further into this direction, consider the configuration shown in Figure 18. Two antenna arrays are shown, each composed of two thin and lossless small dipoles. One array is used for transmission, the other for reception. The dipoles are oriented in the same direction, say parallel to the z-axis. There are two ideal metallic reflection plates placed in the middle between the two arrays and oriented parallel to the y-z-plane. These reflectors ensure that there is multipath transmission and reception, which is necessary to successfully employ multistreaming when the antenna separation within the arrays is small. What is not shown in Figure 18 are the high power amplifiers (HPA), the low-noise amplifiers (LNA), and the two lossless impedance matching multiports which are connected between these amplifiers and the antenna ports at each end of the link, respectively.

We can use the multiport communication theory in order to model this communication scenario as a MIMO system consistent with the governing physics [20]. Because there are three paths (a direct path and two paths over the reflection plates) by which the transmitter can reach the receiver, the matrix $\boldsymbol{Z}_{\mathrm{ART}}$ can be written as the sum of three components:

$$\boldsymbol{Z}_{\mathrm{ART}} = \boldsymbol{Z}_{\mathrm{ART},1} + \boldsymbol{Z}_{\mathrm{ART},2} + \boldsymbol{Z}_{\mathrm{ART},3}$$

where

$$\boldsymbol{Z}_{\mathrm{ART},1} = \frac{\Gamma_0 \mathrm{e}^{-\mathrm{j}kD}}{D}\begin{bmatrix} 1 & 1 \\ 1 & 1 \end{bmatrix}$$

corresponds to the direct path, and can be obtained from (34) setting $\theta_{\mathrm{R}} = \theta_{\mathrm{T}} = \pi/2$ and $\alpha = \Gamma_0 \mathrm{e}^{-\mathrm{j}kD}/D$, where Γ_0 is a constant. For the two paths over the reflectors one can obtain from (33):

$$\boldsymbol{Z}_{\mathrm{ART},2,3} = \frac{-\Gamma_0 \mathrm{e}^{-\mathrm{j}kr}}{r}\begin{bmatrix} \mathrm{e}^{\pm \mathrm{j}kd\cos\phi} & 1 \\ 1 & \mathrm{e}^{\mp \mathrm{j}kd\cos\phi} \end{bmatrix},$$

where r is the distance from the center of the transmitter's array to the center of the receiver's array, taking the longer way over the reflection plates $(r = D/\sin\phi)$. The minus sign in front of the constant Γ_0 is due to the reflected waves having to change their phase by 180 degrees, because the incident field is polarized *tangential* to the reflectors. Assuming, for simplicity, that the dipoles are Hertzian dipoles, the real-parts of the receive and transmit impedance matrices can be obtained from (28). By virtue of (27), the channel matrix, $\boldsymbol{H} \in \mathbb{C}^{2\times 2}$, of the corresponding MIMO system model

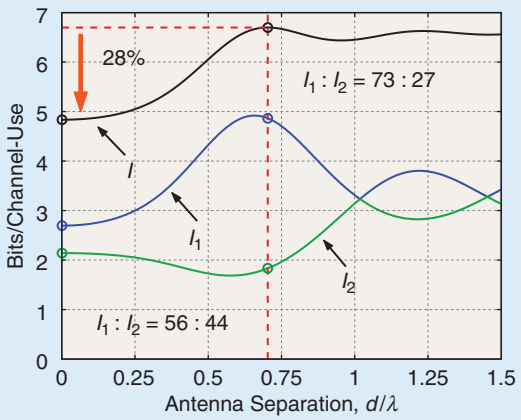

Figure 19. Mutual information for the two data-streams.

$$\boldsymbol{y} = \boldsymbol{H}\boldsymbol{x} + \boldsymbol{\vartheta}, \quad P_{\mathrm{Tx}} = \mathrm{E}[\|\boldsymbol{x}\|_2^2], \quad \mathrm{E}[\boldsymbol{\vartheta}\boldsymbol{\vartheta}^{\mathrm{H}}] = \sigma^2 \mathbf{I},$$

can then be computed. One can write the singular value decomposition of $\boldsymbol{H}$ as

$$\boldsymbol{H} = \boldsymbol{U}\begin{bmatrix} \mu_1 & 0 \\ 0 & \mu_2 \end{bmatrix}\boldsymbol{V}^{\mathrm{H}},$$

where the two unitary matrices $\boldsymbol{U}$ and $\boldsymbol{V}$ contain the left- and right-hand side singular vectors, respectively, and $\mu_1 \geq \mu_2 \geq 0$ are the corresponding singular values. With the bijective transformations $\hat{\boldsymbol{y}} = \boldsymbol{U}^{\mathrm{H}}\boldsymbol{y}$, and $\hat{\boldsymbol{x}} = \boldsymbol{V}^{\mathrm{H}}\boldsymbol{x}$, one obtains with

$$\hat{y}_i = \mu_i \hat{x}_i + \hat{\vartheta}_i, \quad P_{\mathrm{Tx}} = \sum_i \mathrm{E}[|\hat{x}_i|^2], \quad \mathrm{E}[\hat{\vartheta}_i \hat{\vartheta}_j^*] = \sigma^2 \delta_{i,j},$$

where $i,j \in \{1,2\}$ two systems which can be operated simultaneously without interfering with each other. Assuming that the noise is Gaußian distributed, it follows from the $\hat{\vartheta}_i$ being uncorrelated that they are also statistically independent. Therefore, one obtains two information theoretically independent complex additive white Gaußian noise (AWGN) channels over which one can transfer information simultaneously. Using Shannon's formula for the channel capacity [43] of a complex AWGN channel, the channel capacity, C, of the system of the two channels is given by the sum of their individual channel capacities. The only degree of freedom left is the split of power, so that:

$$C = \max_{P_1,P_2} \sum_{i=1}^{2} \log_2(1 + \mu_i^2 P_i/\sigma^2), \text{ such that } \sum_{i=1}^{2} P_i \leq P,$$

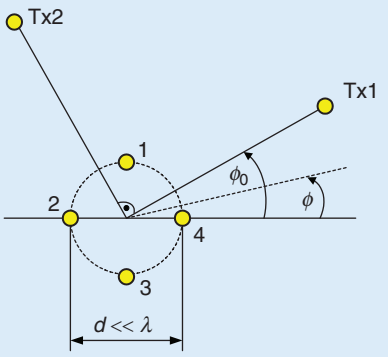

Figure 20. MAC formed by two independent transmitters (Tx1, Tx2), and a compact 4-antenna receiver in empty space.

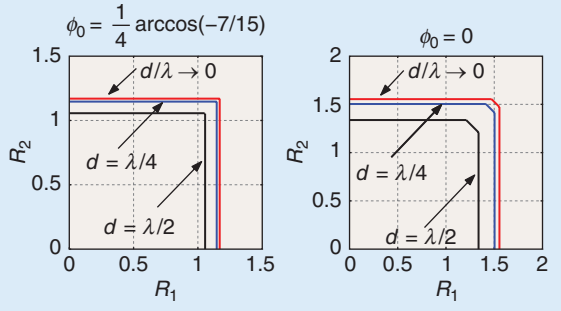

Figure 21. The capacity regions of the system shown in Figure 20, for three different diameters of the antenna array, and two different positions of the users ($\phi_0 \in \{(1/4)\arccos(-7/15), 0\}$).

where P is the available transmit power, and $P_i = \mathrm{E}[|\hat{x}_i|^2]$. The optimum power split (P_1, P_2) is given by the *waterfilling* solution [44]. This solution has the property that, for small values of P, the stronger of the two channels (the one with the larger μ_i) is assigned the whole available power, switching off the second channel completely. Only when there is sufficient power available, will the weaker channel get a share. Asymptotically, for large powers, the waterfilling solution approaches an equal split of the power, regardless of the strength of the channel.

Our focus here, however, is more on the channel quality (quantified by the μ_i), and we would like to avoid the waterfilling algorithm's power-level dependent favorization of one channel. We therefore set the power levels to be equal and obtain the mutual information for the MIMO channel as:

$$I = I_1 + I_2, \quad \text{where} \quad I_i = \log_2\left(1 + \mu_i^2 \frac{P/2}{\sigma^2}\right).$$

Note that $I_1 \geq I_2$ due to $\mu_1 \geq \mu_2$. The results for these mutual information is shown in Figure 19. As the antenna separation d is reduced, the total mutual information, I, reduces. However, this reduction is *not* because the weaker stream would break down as d/λ approaches zero. On the contrary, as d is decreased from about 0.58λ, the weaker stream's mutual information actually *increases.* In fact, for small values of d/λ, it contributes a substantial amount (about 44%) to the sum mutual information.

D. Multiple Access

In a multiple access channel (MAC), some number of independent transmitters communicate simultaneously with a receiver while using the same band of frequencies. Information theory characterizes a MAC by its capacity region [30], the set of all rate-tuples which can be supported simultaneously. Consider, for instance, the Gaußian MAC with two independent single-antenna transmitters, where

$$\boldsymbol{y} = \boldsymbol{h}_1 x_1 + \boldsymbol{h}_2 x_2 + \boldsymbol{\vartheta} \tag{39}$$

is the received signal vector, $\boldsymbol{\vartheta}$ is additive white Gaußian noise (AWGN), x_1 and x_2 are the independent Gaußian transmit signals, while $\boldsymbol{h}_1$ and $\boldsymbol{h}_2$ are the M-dimensional channel vectors, and M is the number of receiver antennas. The capacity region of this Gaußian MAC is given by the following three inequalities [30]:

$$0 \leq R_i \leq \log_2\left(1 + \frac{P}{\sigma^2}\|\boldsymbol{h}_i\|_2^2\right), \quad i \in \{1, 2\}, \tag{40}$$

$$R_1 + R_2 \leq \log_2 \det\left(\mathbf{I} + \frac{P}{\sigma^2}\boldsymbol{H}^{\mathrm{H}}\boldsymbol{H}\right), \quad \boldsymbol{H} = [\boldsymbol{h}_1 \ \ \boldsymbol{h}_2]. \tag{40a}$$

For simplicity, it is assumed that both users transmit with the same power P. The first two inequalities (40) assert that the achievable data rates R_i for each user cannot exceed the channel capacity they would have, if the other user was quiet. (The users do not co-operate in any way in a MAC). The third inequality (40a) states that the sum of the achievable rates cannot exceed the channel capacity that would result if the two users co-operated and formed a $M \times 2$ MIMO system. One can see that (40a) is redundant if and only if $\boldsymbol{h}_2^{\mathrm{H}}\boldsymbol{h}_1 = 0$. Only then can each user reliably transfer information at the same rate as if it was the only user.

This MAC can serve as a model for a space-division multiple access (SDMA) system, were only the receiver is equipped with multiple (M) antennas [45]. To be concrete, consider the system shown in Figure 20. Here $M = 4$ antennas are placed to form a uniform circular array. The two users are located in the same plane as the array at azimuthal angles ϕ_0 and $\phi_0 + \pi/2$, respectively. The propagation environment shall be empty space. By virtue of (27), the system from Figure 20 can be modeled as the MAC defined in (39). Assuming that the two transmitters are separated far enough that their mutual

Did we get the physics right in the modeling of multichannel communication systems? This question was the starting point of the investigations reported here which have lead to quite a number of interesting insights and results.

interaction is negligible, the system can be split into two independent systems, one for each user. With the help of (33), one can then write for those two systems:

$$\boldsymbol{Z}_{\mathrm{ART},1} = \alpha \boldsymbol{a}(\phi_0), \quad \boldsymbol{Z}_{\mathrm{ART},2} = \alpha \boldsymbol{a}(\phi_0 + \pi/2),$$

where

$$\boldsymbol{a}(\phi) = \begin{bmatrix} \exp\left(\mathrm{j}\frac{1}{2}kd\sin\phi\right) \\ \exp\left(-\mathrm{j}\frac{1}{2}kd\cos\phi\right) \\ \exp\left(-\mathrm{j}\frac{1}{2}kd\sin\phi\right) \\ \exp\left(\mathrm{j}\frac{1}{2}kd\cos\phi\right) \end{bmatrix}.$$

Assuming all antennas are isotropic radiators, $\mathrm{Re}\{\boldsymbol{Z}_{\mathrm{AR}}\}$ is proportional to matrix $\boldsymbol{C}$ from (32), where the distances $d_{m,n}$ can easily be obtained from the array geometry in Figure 20. With (27) then follows:

$$\boldsymbol{h}_1 = \xi \boldsymbol{C}^{-1/2}\boldsymbol{a}(\phi_0), \quad \boldsymbol{h}_2 = \xi \boldsymbol{C}^{-1/2}\boldsymbol{a}(\phi_0 + \pi/2),$$

where ξ is a constant. Using (40) and (40a) one can then compute the capacity region of the system of Figure 20. Three such regions are shown in Figure 21 for different antenna spacing d/λ, while the ratio P/σ^2 is kept constant.

As can be observed from Figure 21, a compact size of the receiver's antenna array does *not* necessarily impair the capacity region of a Gaußian multiple access channel. On the contrary, it is the *smallest* arrays (much smaller than half of the wavelength) which offer the *largest* capacity region for the same transmit power. For certain user positions, it is even possible to obtain a rectangular capacity region despite the fact that the receiver's uniform circular array has a much smaller diameter than half the wavelength.

VI. Conclusion

»Did we get the physics right in the modeling of multichannel communication systems?« This question was the starting point of the investigations reported here which have lead to quite a number of interesting insights and results. A multi-antenna radio communications system has to be modeled by linear multiports to enable consistency with the underlying physics. As shown, computation of transmit power or receiver noise covariance requires knowledge of the governing physics. Circuit theory is shown to be the perfect link to bridge the gap between electromagnetic theory, information theory, and signal processing. Therefore, it has become clear that circuit theory is not only of fundamental importance for the detailed design of individual components of a communication system (such as amplifiers, mixers, matching circuits, analog/digital and digital/analog converters, to name a few), but it is crucial for the *overall conceptual design*, where one has to decide on the number of antennas and the sizes of the arrays, and evaluate performance measures in different areas, such as coverage, link quality, information rate and multi-user capacity regions. The multiport theory of communication provides the perfect framework for such conceptual design decision.

Michel T. Ivrlač received his first Dipl.-Ing. degree in electrical engineering from the Munich University of Applied Sciences, in 1994. He earned the second Dipl.-Ing. degree and the Dr.-Ing. degree in electrical engineering and information technology from the Technische Universität München (TUM) in 1998 and 2005, respectively. He presently holds the position of a senior researcher with the Institute for Circuit Theory and Signal Processing at TUM, where he is teaching courses on circuit theory and communication. His main research interests are the physics of communications, signal processing for cellular networks, and coding for ultra high speed communications. He lives with his wife and children in Munich, Germany.

Josef A. Nossek earned the Dipl.-Ing. degree and the Dr. techn. degree, both in electrical engineering, from University of Technology in Vienna, Austria in 1974 and 1980, respectively. He joined the Siemens AG, Munich, Germany, in 1974, where he was engaged in the design of both passive and active filters for communication systems. In 1978, Josef A. Nossek became Supervisor, and in 1980, Head of a group of labs engaged in designing monolithic filters (analog and digital). Since 1982, he has been the Head of a group of labs designing digital radio systems with the Transmission Systems Department of Siemens AG. In 1984, he was a Visiting Professor at the University of Capetown. From 1987 till 1989, Josef A. Nossek was Head of the Radio Systems Design Department, where he was instrumental in

introducing high speed VLSI signal processing into digital microwave radio. Since April 1989, he has been a Professor of circuit theory and design at the Munich University of Technology (TUM), where he teaches undergraduate and graduate courses in the field of circuit and system theory, and he leads research on signal processing algorithms in communications, especially multiantenna communication systems. Josef A. Nossek was President Elect, President and Past President of the IEEE Circuits and Systems Society in the years 2001, 2002, and 2003, respectively. He was Vicepresident of VDE (Verband der Elektrotechnik, Elektronik und Informationstechnik e.V.) 2005, and 2006, and was President of VDE in 2007, and 2008. His awards include the ITG Best Paper Award 1988, the Mannesmann Mobilfunk (now Vodafone) Innovationsaward 1998, the Award for Excellence in Teaching from the Bavarian Ministry for Science, Research and Art in 1998. From the IEEE Circuits and Systems Society he received the Golden Jubilee Medal for »Outstanding Contributions to the Society« in 1999, and the Education Award in 2008. Josef A. Nossek was awarded the »Bundesverdienstkreuz am Bande«, in 2008. In 2009, he became elected member of Acatech.

References

[1] R. P. Feynman, *The Character of Physical Law*. New York: Random House, 1994.

[2] A. Sommerfeld, *Vorlesungen Über Theoretische Physik, Band I—Mechanik*. Thun, Frankfurt am Main: Verlag Harri Deutsch, 1994.

[3] L. Landau and E. Lifshitzs, *Course of Theoretical Physics, Volume I—Mechanics*. Burlington, MA: Butterworth-Heinemann, 1979.

[4] T. Cover and J. Thomas, *Elements of Information Theory*. New York: Wiley, 1991.

[5] L. Scharf, *Statistical Signal Processing*. Reading, MA: Addison-Wesley, 1991.

[6] J. Proakis, *Digital Communications*. New York: McGraw-Hill, 1995.

[7] A. Oppenheim, A. Willsky, and S. Nawab, *Signal and Systems*. Englewood Cliffs, NJ: Prentice-Hall, 1983.

[8] V. Belevitch, *Classical Network Theory*. San Francisco, CA: Holden Day, 1968.

[9] H. Callen and T. Welton, "Irreversibility and generalized noise," *Phys. Rev.*, vol. 83, no. 1, July 1951.

[10] A. Lapidoth, *A Foundation in Digital Communicatiossn*. Cambridge, U.K.: Cambridge Univ. Press, 1995.

[11] J. G. Proakis and D. G. Monolakis, *Digital Signal Processing*, 2nd ed. New York: Macmillan, 1992.

[12] R. Q. Twiss, "Nyquist's and Thevenin's theorems generalized for nonreciprocal linear networks," *J. Appl. Phys.*, vol. 26, pp. 599–602, May 1955.

[13] J. W. Wallace and M. A. Jensen, "Mutual coupling in MIMO wireless systems: A rigorous network theory analysis," *IEEE Trans. Wireless Commun.*, vol. 3, no. 4, pp. 1317–1325, July 2004.

[14] C. Findeklee, "Array noise matching; generalization, proof and analogy to power matching," *IEEE Trans. Antennas Propag.*, vol. 59, no. 2, pp. 452–459, 2011.

[15] K. F. Warnick and M. A. Jensen, "Optimal noise matching for mutually coupled arrays," *IEEE Trans. Antennas Propag.*, vol. 55, pp. 1726–1731, June 2007.

[16] M. Ivrlač and J. Nossek, "On the physical meaning of the model of two uncoupled isotrops," in *ITG Workshop Smart Antennas (WSA2012)*, Dresden, Germany, Mar. 2012.

[17] H. T. Friis, "Noise figure of radio receivers," *Proc. IRE*, vol. 32, pp. 419–422, July 1944.

[18] H. Hillbrand and P. Russer, "An efficient method for computer aided noise analysis of linear amplifier networks," *IEEE Trans. Circuits Syst.*, vol. 23, no. 4, pp. 235–238, June 1976.

[19] M. T. Ivrlač and J. A. Nossek, "Toward a circuit theory of communication," *IEEE Trans. Circuits Syst. I*, vol. 57, no. 7, pp. 1663–1683, July 2010.

[20] M. Ivrlač and J. A. Nossek, "On multi-streaming with compact antenna arrays," in *Proc. ITG Int. Workshop Smart Antennas,* Aachen, Germany, Feb. 2011.

[21] J. D. Jackson, *Classical Electrodynamics*. New York: Wiley, 1998.

[22] H. Yordanov, M. T. Ivrlač, P. Russer, and J. A. Nossek, "Arrays of isotropic radiators—A field-theoretic justification," in *Proc. IEEE/ITG Int. Workshop Smart Antennas,* Berlin, Germany, Feb. 2009.

[23] A. Balanis, *Antenna Theory*, 2nd ed. New York: Wiley, 1997.

[24] S. A. Schelkunoff and H. T. Friis, *Antennas. Theory and Practice*. New York: Wiley, 1952.

[25] K. Kahn and H. Kurss, "Minimum-scattering antennas," *IEEE Trans. Antennas Propag.*, vol. AP-13, pp. 671–675, Sept. 1965.

[26] W. Wasylkiwskyj and W. K. Kahn, "Theory of mutual coupling among minimum-scattering antennas," *IEEE Trans. Antennas Propag.*, vol. 18, no. 2, pp. 204–216, Mar. 1970.

[27] ETSI, *Universal Mobile Telecommunications System (UMTS); Spatial Channel Model for Multiple Input Multiple Output (MIMO) Simulations*, 3GPP TR 25.996 version 11.0.0 Release 11, Sept. 2012.

[28] M. Ivrlač and J. Nossek, "Quantifying diversity and correlation in Rayleigh fading MIMO communication systems," in *Proc. 3rd IEEE Int. Symp. Signal Processing Information Technology (ISSPIT)*, Dec. 2003.

[29] I. E. Telatar, "Capacity of multi-antenna Gaussian channels," *Eur. Trans. Telecommun.*, vol. 10, no. 6, pp. 585–596, Nov. 1999.

[30] D. Tse and P. Viswanath, *Fundamentals of Wireless Communication*. Cambridge, U.K.: Cambridge Univ. Press, 2005.

[31] A. I. Uzkov, "An approach to the problem of optimum directive antennae design," *Comptes Rendus (Doklady) de l'Académie des Sciences de l'URSS*, vol. 53, no. 1, pp. 35–38, 1946.

[32] S. A. Schelkunoff, "A mathematical theory of linear arrays," *Bell Systems Tech. J.*, vol. 22, pp. 80–87, Jan. 1943.

[33] N. Yaru, "A note on super-gain arrays," *Proc. IRE*, vol. 39, pp. 1081–1085, Sept. 1951.

[34] D. Johnson and D. Dudgeon, *Array Signal Processing*. Englewood Cliffs, NJ: Prentice-Hall, 1991.

[35] M. T. Ivrlač and J. A. Nossek, "High-efficiency super-gain antenna arrays," in *Proc. ITG Int. Workshop Smart Antennas,* Bremen, Germany, Feb. 2010.

[36] E. E. Altshuler, T. H. O'Donnell, A. D. Yaghjian, and S. R. Best, "A monopole superdirective array," *IEEE Trans. Antennas Propag.*, vol. 53, no. 8, pp. 2653–2661, Aug. 2005.

[37] J. C. Liberti and T. S. Rappaport, *Smart Antennas for Wireless Communications*. Englewood Cliffs, NJ: Prentice-Hall, 1999.

[38] D. S. Shiu, G. J. Foschini, M. J. Gans, and J. M. Kahn, "Fading correlation, and its effect on the capacity of multi-element antenna systems," *IEEE Trans. Commun.*, vol. 48, no. 3, pp. 502–512, 2000.

[39] J. S. Hammerschmidt and C. Brunner, "The implications of array and multipath geometries in spatial processing," in *Proc. IEEE/IEE Int. Conf. Telecommunications*, Acapuloco, Mexico, May 2000.

[40] M. Ivrlač and J. Nossek, "On the diversity performance of compact arrays," in *Proc. 30th General Assembly Union Radio Science (URSI2011)*, Istanbul, Turkey, Aug. 2011.

[41] H. Chaloupka and X. Wan, "Novel approach for diversity and MIMO antennas at small mobile platforms," in *Proc. IEEE Int. Symp. Personal, Indoor Mobile Radio Communications (PIMRC)*, 2004.

[42] A. Knopp, R. Schwarz, B. Lankl, D. Ogermann, and C. Hofmann, "Satellite system design examples for maximum MIMO spectral efficiency in LOS channels," in *Proc. Global Communications Conf. 2008 (GLOBECOM08)*, New Orleans, LA, Nov. 2008.

[43] C. E. Shannon, "A mathematical theory of communications," *Bell Syst. Tech. J.*, vol. 27, pp. 379–423, 623–656, July 1948.

[44] R. Gallager, *Information Theory and Reliable Communication*. New York: Wiley, 1968.

[45] M. Ivrlač and J. Nossek, "Gaussian multiple access channel with compact antenna arrays," in *2011 IEEE Int. Symp. Information Theory (ISIT11)*, St. Petersburg, Russia., Aug. 2001.